

Earthquake risk assessment of seismically isolated extradosed bridges with lead rubber bearings

Dookie Kim[†]

*Department of Civil and Environmental Engineering, Kunsan National University,
Kunsan, Jeonbuk 573-701, Korea*

Jin-Hak Yi[‡]

*Coastal Engineering Research Department, Korea Ocean Research and Development Institute,
Ansan, Gyeonggi 426-744, Korea*

Hyeong-Yeol Seo^{‡†}

*Department of Civil and Environmental Engineering, Kunsan National University,
Kunsan, Jeonbuk 573-701, Korea*

Chunho Chang^{‡‡}

Department of Civil Engineering, Keimyung University 1000 Sindang, Dalseo, Daegu 704-701, Korea

(Received May 10, 2007, Accepted June 24, 2008)

Abstract. This study presents a method to evaluate the seismic risk of an extradosed bridge with seismic isolators of lead rubber bearings (LRBs), and also to show the effectiveness of the LRB isolators on the extradosed bridge, which is one of the relatively flexible and lightly damped structures in terms of seismic risk. Initially, the seismic vulnerability of a structure is evaluated, and then the seismic hazard of a specific site is rated using an earthquake data set and seismic hazard maps in Korea. Then, the seismic risk of the structure is assessed. The nonlinear seismic analyses are carried out to consider plastic deformation of bridge columns and the nonlinear characteristics of soil foundation. To describe the nonlinear behaviour of a column, the ductility demand is adopted, and the moment-curvature relation of a column is assumed to be bilinear hysteretic. The fragility curves are represented as a log-normal distribution function for column damage, movement of superstructure, and cable yielding. And the seismic hazard at a specific site is estimated using the available seismic hazard maps. The results show that in seismically-isolated extradosed bridges under earthquakes, the effectiveness of the isolators is much more noticeable in the columns than the cables and girders.

Keywords: seismic fragility; seismic hazard; seismic risk; LRB seismic isolator; extradosed bridge.

[†] Assistant Professor, E-mail: kim2kie@kunsan.ac.kr

[‡] Senior Research Scientist, Corresponding author, E-mail: yijh@kordi.re.kr

^{‡†} Ph.D., E-mail: hojins97@paran.com

^{‡‡} Assistant Professor, E-mail: chunho@kmu.ac.kr

1. Introduction

Recently, many researches to assess seismic damages of a structure are being developed. Seismic performance assessment of civil infra-structures such as bridges, buildings, nuclear power plants and offshore structures is very important because the seismic damages of these structures may bring not only economic loss but also loss of human lives (Su *et al.* 2002).

The seismic performance of a bridge can be evaluated using the nonlinear time history analysis or the nonlinear static analysis (in other words, pushover analysis) such as the capacity spectrum method based on the design response spectrum, and so on (Chung *et al.* 2006, Elnashai 2001). Nonlinear analysis techniques are getting more popular owing to the development of high-performance computational devices. However, these conventional methods are usually carried out in the deterministic domain, and therefore it is difficult to consider the uncertainties of seismic events such as duration, frequency components and seismic intensity.

To overcome this shortcoming of the conventional deterministic approaches, this paper presents probabilistic seismic risk assessment (PSRA) of a structure considering uncertainties of earthquake occurrences. In order to evaluate the seismic risk of a structure, seismic fragility as an index of the seismic vulnerability of a structure and the seismic hazard as a measure of the earthquake intensity at the specific site are to be combined.

Seismic fragility was first introduced to the probabilistic seismic safety assessment of nuclear power plants in the 1980's (Kennedy and Ravindra 1984), and was recently accepted as a reliable method for the evaluation of the seismic performance of civil infra-structures, such as bridges and buildings (Shinozuka *et al.* 2002). Seismic fragility curves generally show the probability of seismic damage at specified levels versus the ground motion index such as peak ground acceleration (PGA) and peak ground velocity (PGV). While the fragility curve usually takes the PGA value as the ground motion index, Karim and Yamazaki (2001) recently performed an analysis taking the PGV as well and compared the results with those using PGA. For bridge structures, seismic fragility has been studied using various damage indices such as pier ductility, displacement of bearing, and the damage index of Park and Ang (Ghobarah *et al.* 1997). Fragility analysis has been performed for retrofitted bridges as well (Kim and Shinozuka 2004).

Seismic risk describes the potential for damage or losses that a region is prone to experience resulting from a seismic event. This is in contrast to seismicity which describes the recurrence rate of earthquakes with different magnitudes and seismic hazards which quantify the recurrence rates of different ground motions. Seismic risk can also be defined as the spatially and temporally integrated product of the seismic hazard, the value of assets and the fragility of assets (Jacob 1992). For the seismic hazard analysis, the seismic hazard maps of Korea are utilized to read the PGA values corresponding to various return periods for a given site, and the probability density function of the PGA is calculated using a probabilistic approach.

The seismic fragility analysis has been commonly carried out to calculate the probability of structural damage versus the ground surface motion to which the structure is subjected. Hence in this study, artificial earthquakes are generated according to the design response spectrum given for the rock outcrop; and the acceleration time history at the surface ground are then evaluated considering the site amplification effects according to the site condition, since the seismic hazard map is constructed based on the rock outcrop motion.

The seismic risk of a bridge, isolated using lead rubber bearings (LRBs) of a circular section, is evaluated herein. An extradosed bridge with a 6-span continuous concrete deck is utilized as an

example structure. In this study, the rotational ductility of a column, the displacement of a superstructure and the cable yielding are considered as possible types of seismic damage. Generally, the LRBs have not been considered as an effective tool to improve the seismic performance of flexible and lightly damped structures including extradosed bridges because these bridges have relatively long natural periods. In this study, the effectiveness of LRBs on extradosed bridges is verified using a probabilistic seismic risk.

2. Design of LRB seismic isolator

Seismically-isolated structure is designed for exceeding the earthquake dominant period, which is enabled by making its natural period artificially longer than the seismic dominant periods (Fig. 1). For example, in the case of a bridge structure with a short period, the natural period of a structure can be increased by installing the seismic isolator at the bottom of the girders (Fig. 2).

The seismic isolator is generally designed using the guidelines such stipulated in AASHTO or UBC (Farzad Naeim *et al.* 2003).

LRB, one of the seismic isolators, behaves as elasto-plastic as shown in Fig. 3, so the seismic force is reduced by shifting the natural period of the structure using the elastic behaviour of rubber, and the seismic energy is absorbed by the plastic behaviour of lead. Therefore, it is very important

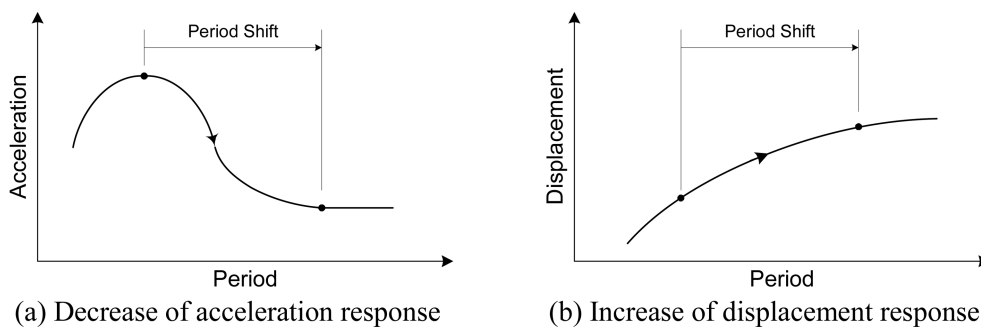


Fig. 1 Seismic response of isolated structures

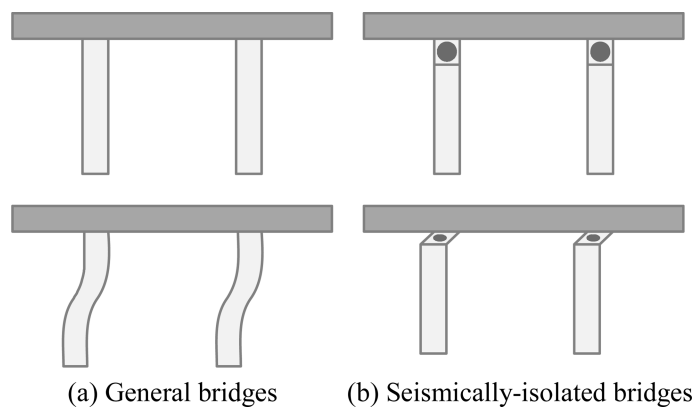


Fig. 2 Comparison on seismic behavior in typical bridges

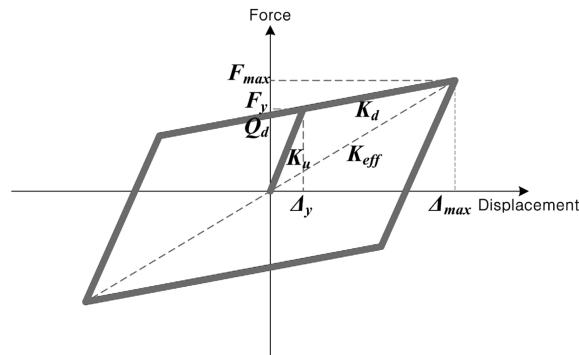


Fig. 3 Properties curves of LRB seismic isolator

to consider how to combine the rubber and the lead in the design of LRB seismic isolators to reduce the seismic force and displacement. In Fig. 3, K_u , K_d and K_{eff} are the initial stiffness, the stiffness after yielding and the effective stiffness of LRB seismic isolators, respectively, Q_d is the yield strength of LRB, F_y and F_{max} are the initial yield and the maximum horizontal forces, respectively, and Δ_y and Δ_{max} are the yield and maximum displacements of LRB seismic isolator, respectively.

The main purpose of the seismic isolator design is to reduce the seismic force by shifting the natural period of a structure to the long period range. Ghobarah and Ali (1998) recommended that the isolator design starts by deciding K_u and K_d to shift the natural period of a bridge and determine the yield strength of lead (Q_d) to impose additional damping of about 5% of the total weight of a structure.

However, in cases of flexible structures such as an extradosed bridge or a cable stayed bridge, this concept of seismic isolation is very difficult to apply as these kinds of bridges already have periods beyond the peak seismic period range. Moreover, it is also very difficult to impose additional damping for the yielding of lead because these bridges are very lightly damped structures. Ali and Abdel-Ghaffar (1995) tried to apply the LRBs for seismic isolation of flexible and lightly damped structures, but it has never been clearly recommended for extradosed or cable-stayed bridges. The design parameters of the LRB seismic isolator can be established to minimize the response and installation costs of the bridge. From this point of view, the effectiveness of seismic isolators is quantitatively evaluated by using probabilistic seismic risk assessment.

3. Assessment of seismic risk

3.1 Introduction

Seismic events inevitably involve high levels of uncertainties such as the magnitude, frequency contents, and duration. It is more preferable to deal with the seismic events as probabilistic ones than as deterministic ones. Therefore, the seismic performance of a structure can be reasonably evaluated considering the probabilistic properties of seismic events. The structural vulnerability can be probabilistically evaluated by seismic fragility analysis, and the site hazard can be evaluated using seismic hazard analysis. Then, the seismic risk of a structure on the given construction site

can be assessed by combining the seismic fragility curves and seismic hazard curves. Seismic fragility curves are obtained using Monte Carlo simulation with a set of input ground motion data (Shinozuka *et al.* 2000).

3.2 Seismic fragility analysis

In this study, the seismic fragility curves are expressed in the form of two-parameter log-normal distribution functions as follows. The median (c_k) and the log-standard deviation (ζ_k) of each lognormal distribution are evaluated with the aid of the maximum likelihood estimation. The fragility curve for the k^{th} damage state $F_k(a)$, takes the following form

$$F_k(a) = \Phi\left[\frac{\ln(a/c_k)}{\zeta_k}\right] \tag{1}$$

where a is a PGA value of the earthquake motion, and $\Phi(\cdot)$ is the standard normal distribution function. The likelihood function for the present purpose can be taken as

$$L = \prod_{i=1}^N [F_k(a_i)]^{x_i} \cdot [1 - F_k(a_i)]^{1-x_i} \tag{2}$$

where $x_i = 1$ or 0 depending on whether the bridge sustains the k^{th} damage state under the ground motion with $\text{PGA} = a_i$, and N is the number of input ground motion data. Two parameters c_k and ζ_k in Eq. (1) are computed by maximizing the log-likelihood function as

$$\frac{\partial \ln L}{\partial c_k} = \frac{\partial \ln L}{\partial \zeta_k} = 0, \quad k = 1, 2, \dots, N_{\text{state}} \tag{3}$$

3.3 Seismic hazard and risk analyses

For the purpose of seismic risk assessment for a certain period, say the service life, it is required to know the probability of the earthquake occurrence in addition to the fragility curves. In this study, it is assumed that the earthquake occurs in accordance with the Poisson law and Gumbel's extreme distribution of Type II (Shinozuka *et al.* 1984). If a ground shaking that can be considered as an earthquake ($\text{PGA} \geq a_0$) occurs at a rate of λ_E per year at a site of interest, the probability distribution function of the annual maximum $\text{PGA}(A)$, $F_A(a)$, is related to the probability of the PGA of one seismic event (A_1), $F_{A_1}(a)$, as

$$F_A(a) = \exp\{-\lambda_E(1 - F_{A_1}(a))\} \tag{4}$$

Therefore, when a_0 indicates the minimum PGA value to be considered, $F_{A_1}(a_0) = 0$, and hence

$$\lambda_E = -\ln F_A(a_0) \tag{5}$$

Assuming that $F_A(a)$ is of the extreme distribution of Type II, the following can be obtained as

$$F_A(a) = \exp\left\{-\left(\frac{a}{u}\right)^{-\alpha}\right\} \tag{6}$$

Since the seismic hazard map is defined as the PGA levels associated with a return period or an exceedance probability for a certain period of time, the probability distribution of the annual maximum PGA $F_A(a)$ can be obtained from the annual exceedance probability, $P\{A > a\}$, as

$$F_A(a) = 1 - P\{A > a\} \tag{7}$$

The two parameters (α and u) of Eq. (1) can be obtained from a curve fitting to the data in seismic hazard maps for various probability levels. The annual occurrence rate, λ_E , is calculated by Eq. (8), and thus, the probability distribution $F_{A_1}(a)$ of an earthquake and its probability density function $f_{A_1}(a)$ are also calculated as

$$\lambda_E = -\ln F_A(a_0) = \left(\frac{a_0}{u}\right)^{-\alpha} \tag{8}$$

$$F_{A_1}(a) = 1 + \frac{1}{\lambda_E} \cdot \ln F_A(a) = 1 - \left(\frac{a}{a_0}\right)^{-\alpha} \tag{9}$$

$$f_{A_1}(a) = \frac{dF_{A_1}(a)}{da} = (\alpha \cdot a_0^\alpha) \cdot a^{-\alpha-1} \tag{10}$$

Combining Eq. (10) with the fragility curve $F_k(a)$, the seismic risk for the k^{th} damage state due to one occurrence of earthquake, p_f^c , and the seismic risk for n -years, p_f^{n-yr} can be obtained as

$$p_f^c = \int_{a_0}^{a_{\max}} F_k(a) f_{A_1}(a) da \tag{11}$$

$$p_f^{n-yr} = 1 - \exp(-n \cdot \lambda_E \cdot p_f^c) \tag{12}$$

4. Free field analyses

For the seismic analysis of a structure, the soil amplification effect is roughly considered using classification of soils. However, it is also important to significantly consider the site amplification due to the soil characteristics and to input seismic excitations. This is because the seismic waves are usually amplified according to the characteristics of soil layers during propagation from bed rock to the site surface. Depending on the locations, the ground motions for an earthquake can be divided

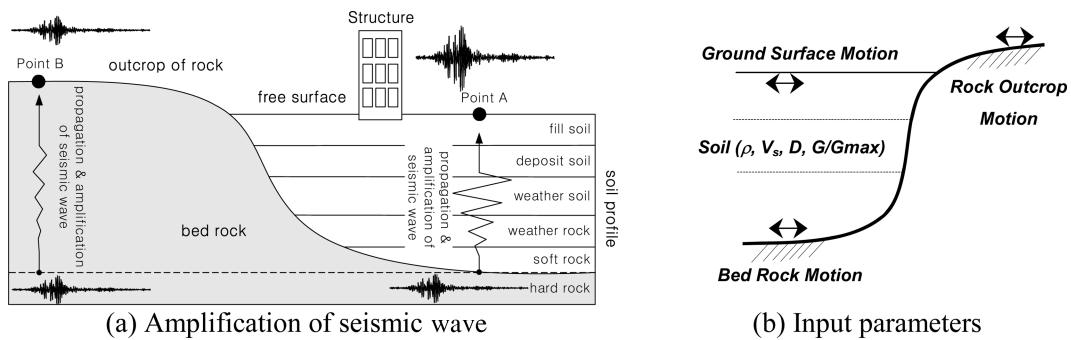


Fig. 4 Free field analyses

into three different phases: rock outcrop motion, bed rock motion, and surface motion, as shown in Fig. 4(a). The design earthquakes in seismic codes are usually defined using the design values at the rock outcrop (AASHTO 1999, KSCE 2005).

In this study, artificial earthquakes are generated according to the design response spectrum given for the rock outcrop, and the acceleration time history at the surface ground are evaluated considering the site amplification effect according to the site condition. Site amplification can be evaluated using several techniques. Among them, the one dimensional free field analysis technique is most widely used. The same technique is incorporated here. In the 1D free field analysis, it is assumed that the seismic response of ground is composed of SH waves propagated in vertical direction from bed rock to the surface, and the soil layers are under half infinite horizontal boundaries.

In general, the ground motions are measurable only on the rock outcrop and on the surfaces. The validity of the free field analyses has been verified by comparing two responses from the real measurement and the numerical analysis (free field analysis) at the surface using the same input rock outcrop motion (Yun *et al.* 1999). There are several available free field analysis programs. One such well-known program, the SHAKE91, utilizes the equivalent linearization algorithm to consider the nonlinear constitutive equation of soils (Idriss and Sun 1992).

In this study, SHAKE91 is used for free field analyses. Relevant input parameters such as mass density (ρ), shear wave velocity (V_s), damping ratio (D), and shear modulus (G/G_{\max}) are shown in Fig. 4(b). It uses the nonlinear deformation characteristics, such as the change of G/G_{\max} and damping ratio (Rechart *et al.* 1970).

5. Seismic risk assessment of an extradosed bridge

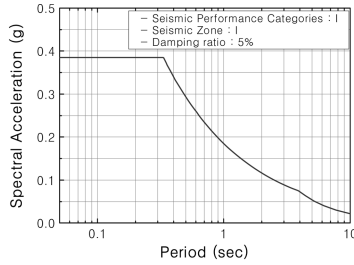
5.1 Generation of artificial earthquakes

In nonlinear time history analysis for earthquakes, it is preferred to take into account the uncertainties related to the earthquake input, such as the magnitude, frequency contents, and duration. Hence, it requires many cases of input ground motions to evaluate the seismic fragility of a bridge. Since only a few measured data are available in Korea a sufficient number of input earthquakes (herein 100 earthquakes) are generated based on the design response spectrum, and then scaled assuming the uniform distribution from 0.005 g to 0.6 g of PGA for input ground motions. To generate the artificial ground motions, the iterative method proposed by Vanmarcke and Gasparini (1976) is used as

$$\ddot{x}_g^1(t) = \left[\Im^{-1} \left\{ \frac{1}{\omega} R(\omega, \xi) e^{j\theta} \right\} \right]_{\text{Re}}, \quad \ddot{x}_g^{n+1}(t) = \Im^{-1} \left\{ \ddot{X}_g^n(\omega) \frac{R(\omega, \xi)}{R^n(\omega, \xi)} \right\} \quad (13)$$

where $\ddot{x}_g^1(t)$ is the ground motion generated at the first iteration from the given design response spectrum $R(\omega, \xi)$, $\ddot{x}_g^{n+1}(t)$ is the ground motion of the $(n+1)$ th iteration, and $R^n(\omega, \xi)$ is the response spectrum calculated from the time history at the n th iteration. θ is a random variable with uniform distribution between 0 and 2π .

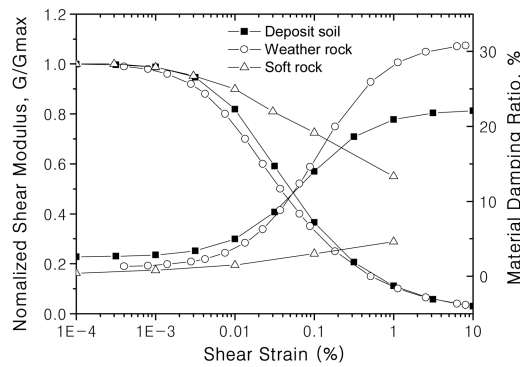
Surface ground motions are generated considering the soil amplification effect using SHAKE91. Fig. 5 shows the procedure for obtaining a surface ground motion from a standard design response



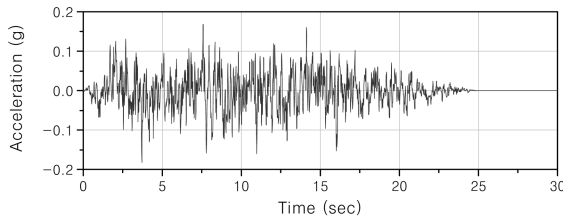
(a) Standard design response spectrum for rock outcrop

Free surface			
Deposit soil	3.0 m	$\rho_1=19.6\text{kN/m}^3$, $G_1=9.16\text{E}4\text{kN/m}^2$, $V_{s1}=300\text{m/sec}$, $D_1=3.0\%$	
Weather rock	1.1 m	$\rho_2=20.6\text{kN/m}^3$, $G_2=1.82\text{E}5\text{kN/m}^2$, $V_{s2}=750\text{m/sec}$, $D_2=3.0\%$	
Soft rock	3.5 m	$\rho_3=23.5\text{kN/m}^3$, $G_3=8.69\text{E}6\text{kN/m}^2$, $V_{s3}=1,840\text{m/sec}$, $D_3=3.0\%$	
Hard rock (outcrop)		$\rho_4=25.5\text{kN/m}^3$, $G_4=1.56\text{E}7\text{kN/m}^2$, $V_{s4}=2,054\text{m/sec}$, $D_4=3.0\%$	

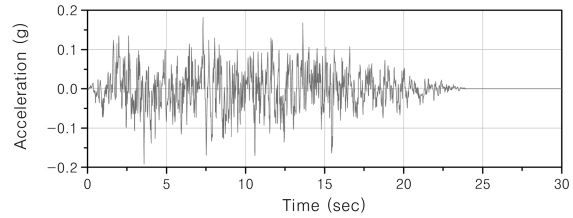
(b) Characteristics of soil layers



(c) Material nonlinearity G/Gmax



(d) Rock outcrop motion



(e) Surface ground motion

Fig. 5 Example of input earthquake

spectrum for rock outcrop by considering the soil characteristics. For a given soil layer, the mean of soil amplification rate is about 1.1 times on the PGA.

5.2 Numerical models for an extradosed bridge

The example extradosed bridge is a six-span continuous concrete girder bridge, with a total length of 670 m, composed of five columns with hollow sections as shown in Fig. 6. The example bridge is designed using the requirement of collapse preventive level under the prescribed return period (1000 years for this bridge), and the design PGA value is 0.154 g. Two cases (Cases I and II) of bearing arrangements are considered: Case I for the typical bridge with general shoes (rollers and hinges) as shown in Fig. 6(a), and Case II for the seismically-isolated bridge with seismic isolators (i.e., LRBs in this study) in Fig. 6(b). In Figs. 6(a) and 6(b) the □, ○ and ⊞ represent “general shoe”, “plastic hinge” and “seismic isolator”, respectively. The column is modelled as an elastic

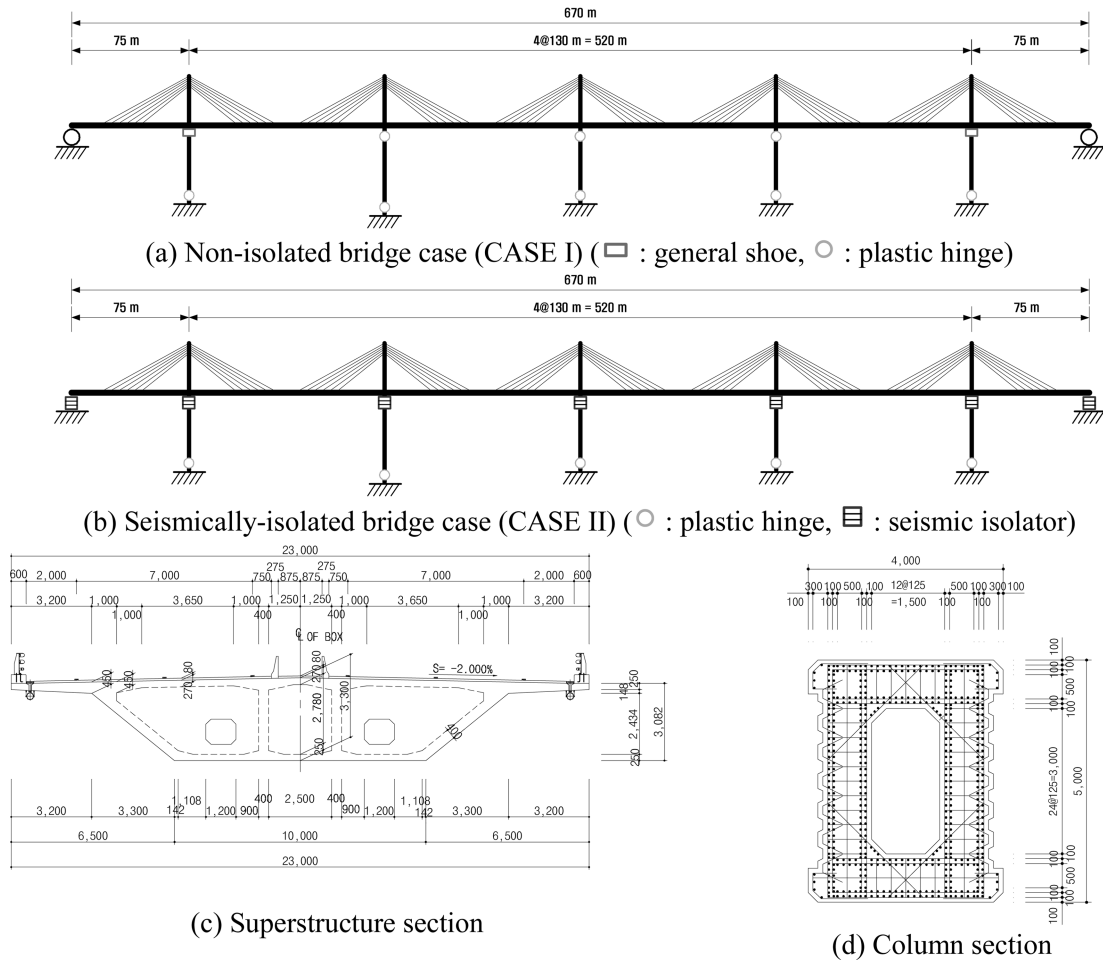


Fig. 6 Bridge models for analysis

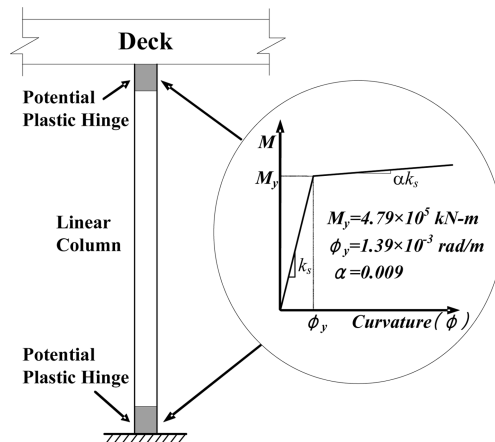


Fig. 7 Elastic-plastic (nonlinear) model of columns

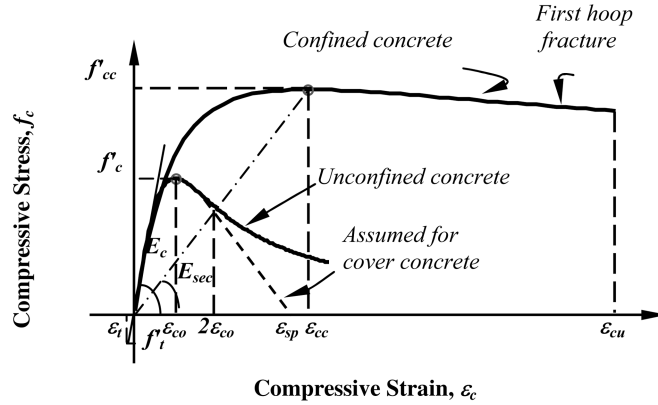


Fig. 8 Stress-strain model for concrete in compression

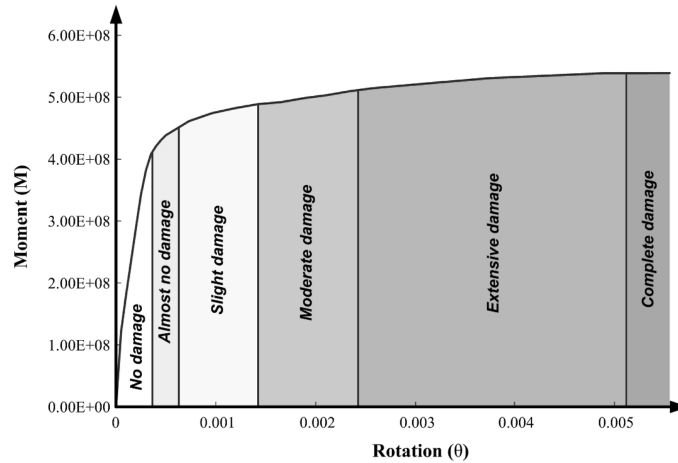


Fig. 9 Moment-rotation curve in plastic hinge

zone with a pair of plastic hinges at each end of the column. The plastic hinge formed in the bridge column is assumed to have bilinear hysteretic characteristics (Fig. 7). The bilinear parameters such as yielding moment and rotation are calculated using the UCFyber based on the stress-strain relationships of concrete in compression as shown in Fig. 8 (Priestley *et al.* 1996, UCFyber Users Manual 2001). 5% viscous damping is considered for the nonlinear seismic analysis. And the additional damping is provided by the hysteretic behavior of LRB isolators during strong earthquakes.

5.3 LRB seismic isolator

Two types of LRB seismic isolators are designed following the equivalent static design method (AASHTO 1999) considering the installation position: i.e., LRBs for abutment part (Type A) and LRBs for column part (Type B). LRBs of type A are installed by one per shoe and two per abutment, while LRBs of type B are installed by four (4) per shoe and eight (8) per column. The sectional properties and design parameters are shown in Fig. 10 and Tables 1 and 2.

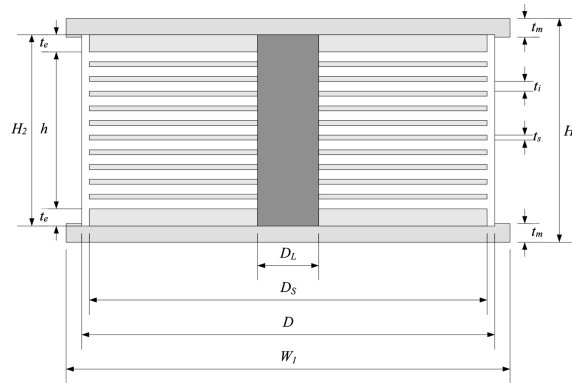


Fig. 10 LRB seismic isolator section

Table 1 Design parameters of LRB seismic isolator

Specification	Symbol	Units	Dimensions	
			Type A	Type B
Widths of the top & bottom steel plate	W_1	Mm	840	1,160
External diameter of LRB	D	Mm	760	1,080
Diameter of the internal reinforcement steel plate	D_s	Mm	720	1,040
Diameter of lead core	D_L	Mm	170	230
Rubber layer total thickness	T_r	Mm	140	140
Rubber layer numbers	n	-	14	14
Thickness of rubber 1 layer	t_i	Mm	10	10
Thickness of the middle internal steel plate	t_s	Mm	4	2.5
Thickness of the top & bottom internal steel plate	t_e	Mm	30	40
Thickness of the top & bottom steel plate	t_m	Mm	38	38
Internal height of the LRB	h	Mm	210	232
Total height of LRB (with conclusion)	H_1	Mm	318	318
Height of LRB (without conclusion)	H_2	Mm	252	252

Table 2 Material properties of LRB seismic isolator

Specification	Symbol	Units	Dimensions	
			Type A	Type B
Design displacement	d_i	cm	6.00	6.00
The first slope stiffness	K_u	kN/cm	221.71	408.78
The second slope stiffness	K_d	kN/cm	18.54	39.63
Yield strength	Q_d	kN	236.42	346.49
Yield force	F_y	kN	258.10	383.67
Yield displacement	Δ_y	m	1.16	0.94
Effective stiffness in design displacement	K_{eff}	kN/cm	57.98	97.41
EDC* in of design displacement	EDC	kN-cm	4573.32	7014.15
Equivalence damping in design displacement	ξ_{eq}	%	34.87	31.85
Vertical stiffness	K_v	kN/cm	23.29	70.63

*EDC : Energy Dissipated per Cycle (area of hysteresis loop)

Table 3 First natural periods of numerical models of the bridge models (units: sec)

Direction	CASE I (Non-isolated bridge)	CASE II (Seismically-isolated bridge)
Horizontal	1.4219	2.2271
Vertical	0.3393	0.3730

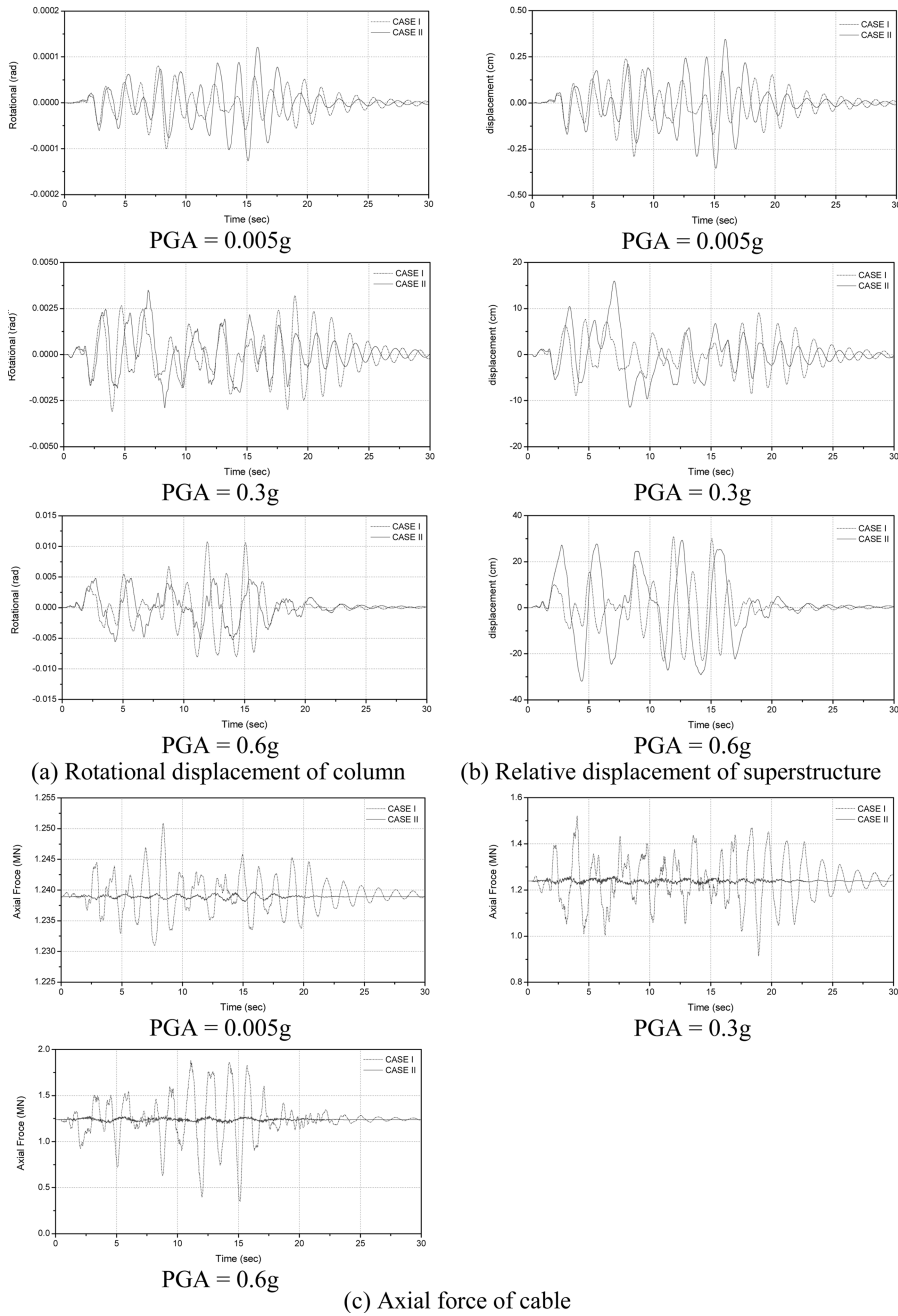


Fig. 11 Seismic responses of an example bridge with and without base isolation

5.4 Seismic fragility analysis

Nonlinear time history analyses are performed for seismic fragility analysis using SAP2000/Nonlinear (Computers and Structures 2002), and 100 artificial earthquakes generated using design response spectrum are used as input earthquakes. Since the EI value for the transverse direction of column is about 5.4×10^8 kN/m² and this is almost 160% of EI value for the longitudinal direction (3.4×10^8 kN/m²), the seismic risk for longitudinal direction is more important and the seismic risk in transverse direction is disregarded in this study. The 1st natural periods for vertical and horizontal directions are compared in Table 3, and it is found that the 1st natural period is significantly increased from 1.42 sec to 2.23 sec for the 1st horizontal mode by adopting the LRBs as the supporting devices. This result contradicts the perception that isolation devices are not so effective in increasing the natural period for extradosed bridges and similar cable stayed bridges. By increasing the natural period, the nonlinear behaviour can be reduced as shown in Fig. 11. Here, the typical responses of the example bridges including the rotational displacement at the bottom of the center pier, the relative displacement of the superstructure at the center and the axial force on the longest cable member in left side of the center pier for three typical PGA levels (0.005 g, 0.3 g and 0.6 g) from nonlinear time history analyses are shown. In the case of responses under the earthquake with PGA of 0.005 g, the maximum amplitudes are not so different and even the maximum amplitude appears to be increased by adopting the LRBs for the relative displacement of superstructure. However, the maximum amplitude of rotational displacement of an isolated bridge is significantly reduced for the earthquake with PGA of 0.6 g. This implies that the LRBs may be more effective for protection of bridges under strong ground motions rather than small scale ground motions. In the case of axial forces on the cable, the maximum axial force can be significantly reduced by introducing LRBs.

The damage states are defined using the rotational ductility of columns following the qualitative description of HAZUS (HAZUS 1997), the relative displacement of superstructure, and the yielding of cables for seismic fragility analysis of an example bridge.

A set of five different damage states are introduced for the seismic damage at columns (Dutta and Mander 1998). Table 4 shows the description of these five damage states and the corresponding drift limits for a typical column. For the purpose of this study, the drift limit can be transformed to peak ductility demand of the columns for each limit state. For the component fragility of superstructure, the relative displacement of the superstructure is evaluated and the limit displacement is set as 6 cm considering the allowable relative displacement in the design specification. The allowable load for the cable elements are determined by adopting 0.6 times the allowable design force, and the value is set as $0.6p_u = 6.2$ MN.

Table 4 Damage states and numbers on the maximum ductility of column

Damage state	Description	Drift limits	Ductility demand	Damage numbers	
				CASE I	CASE II
I (Almost none)	First yield	0.005	1.00	90	87
II (Slight)	Cracking, spalling	0.007	1.60	87	68
III (Moderate)	Loss of anchorage	0.015	3.98	63	9
IV (Extensive)	Incipient column collapse	0.025	6.95	36	1
V (Complete)	Column collapse	0.050	14.40	3	0

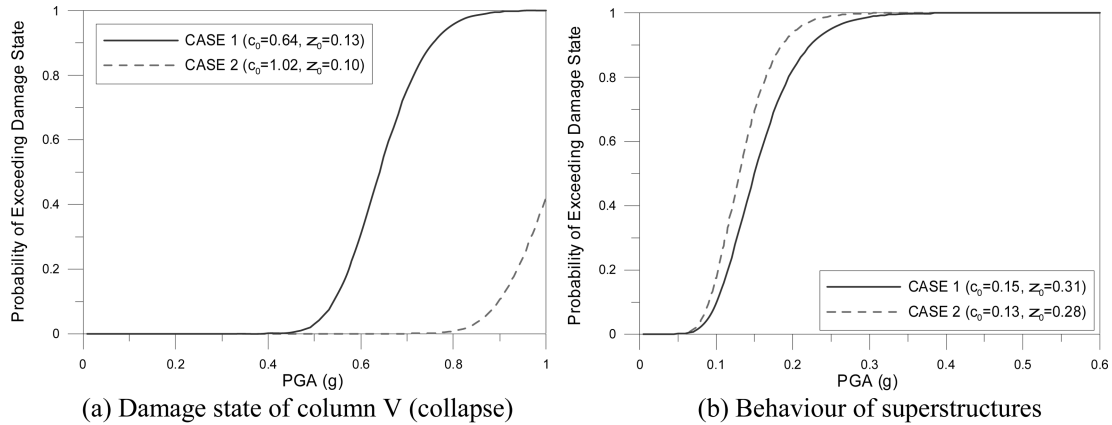


Fig. 12 Seismic fragility curves (Kim *et al.* 2005)

Table 4 lists numbers for the cases exceeding the damage states with and without LRB seismic isolator. From this Table, it can be observed that the number of damaged cases for a seismically-isolated bridge is less than that for a typical bridge owing to the seismic isolation devices. The numbers of damaged cases for moderate and extensive damages (Damage States III and IV) are reduced from 63 to 9 for State III and from 36 to 1 for State IV by replacing the general hinges and rollers with seismic isolation devices. It means that the seismic isolation devices are much more effective for the moderate and extensive seismic damages rather than the slight and almost no damage states. In the case of cable yielding, the maximum axial forces are much less than the allowable value (6.2 MN) as shown in Fig. 11(c). There is no case for cable yielding, and therefore the seismic risk of a bridge in terms of cable yielding is not discussed in the later parts of this study.

Fig. 12 compares seismic fragility curves for an example bridge with typical bearings (Case I) and seismic isolation devices (Case II). Fig. 12(a) shows the fragility curves for column damages while Fig. 12(b) for the seismic damages of the superstructure. From the figures, it can be found that: (1) the median value of the fragility curve for a isolated bridge is shifted from 0.64 to 1.02, which means that the seismic performance of a bridge is enhanced by adopting LRBs as bridge bearings; (2) the median value of fragility curve of a superstructure is slightly reduced from 0.15 to 0.13, and this shows that the superstructure is more susceptible to damages by introducing the LRBs due to allowing large deformation of superstructures.

5.5 Seismic hazard and risk analyses

For the probabilistic seismic risk assessment, the seismic fragility and seismic hazard are to be combined. Seismic hazard on the specific site, where a bridge is located, can be efficiently evaluated using seismic hazard maps in Korea. For the Korean peninsula, the seismic hazard maps have already been constructed through the statistical procedure using historical earthquake data. Therefore the maximum PGA values for a specific return period can be easily read from the seismic hazard maps.

In this study, the seismic hazard maps for the earthquake with 10% exceedance probability for 5, 10, 20, 50, 100, 250 and 1000 years are utilized (EESK 1997). The annual exceedance probability

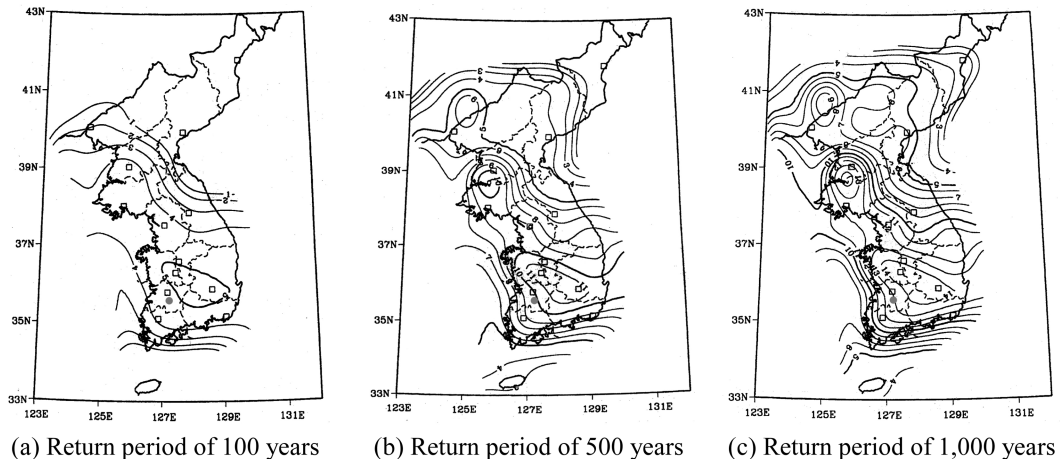


Fig. 13 Seismic hazard maps in Korea (EESK 1997)

(PE_1) can be obtained by converting the exceedance probability of N years (PE_N) as follows

$$PE_1 = 1 - (1 - PE_N)^{1/N} \tag{14}$$

Then, the return period (T) can be obtained by taking the reciprocal value of the annual exceedance probability as

$$T = 1/PE_1 \tag{15}$$

Using Eq. (15), the corresponding return periods for the above-mentioned seismic hazard maps are evaluated as about 50, 100, 200, 500, 1000, 2400, and 4800 years. The obtained maximum PGA values at the field sites for several return periods are summarized in Table 5.

Fig. 14 shows the procedure in determining the values of α and u in Eq. (6). Ultimate distribution of Type II in Eq. (6) can be linearized by taking the logarithmic operation. Then, the regression curve can be obtained using several data of $F_A(a)$ and a , and the probability constants can be estimated as $\alpha = 2.44313$, and $u = 0.00749$. The solid line in Fig. 14 shows the interpolated relation constructed using estimated α and u .

After two parameters (α and u) of Eq. (6) were obtained from a curve fitting to the data, the

Table 5 Exceedance probability of PGA on the return periods

Return period (years)	Exceedance probability per years	PGA
50	10% / 5 years	0.035 g
100	10% / 10 years	0.046 g
200	10% / 20 years	0.068 g
500	10% / 50 years	0.100 g
1000	10% / 100 years	0.130 g
2400	10% / 250 years	0.180 g
4800	10% / 500 years	0.220 g

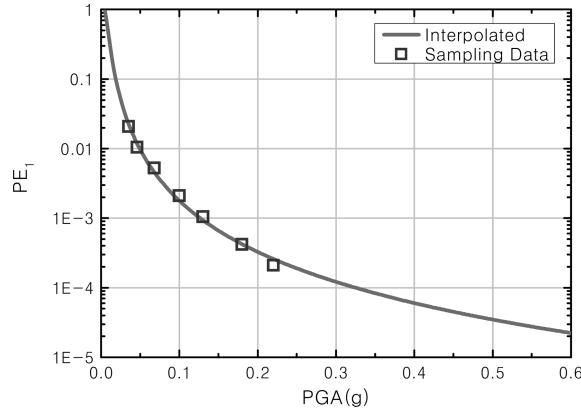


Fig. 14 An annual maximum PGA value (A) and exceeding probability

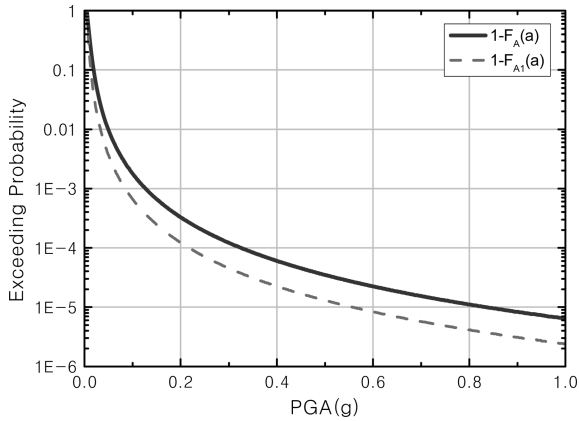


Fig. 15 Exceeding probability for PGA of occurrence earthquake

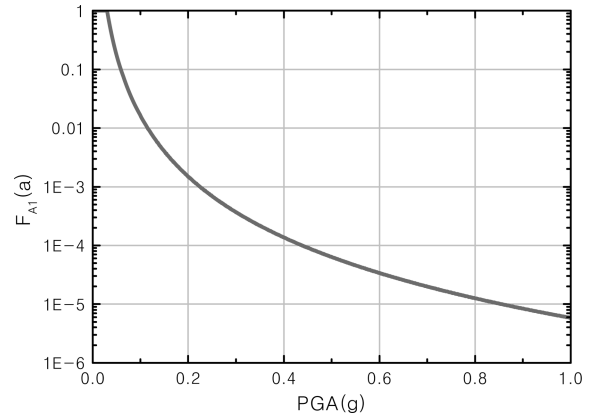


Fig. 16 Seismic hazards for PGA of 1 time occurrence

annual occurrence rate λ_E is then calculated by Eq. (8). When the minimum PGA value a_0 is assumed as 0.005 g, the annual occurrence rate, λ_E , can be evaluated as $\lambda_E = 2.68672$. The probability distribution $F_{A_1}(a)$ of an earthquake and its probability density function $f_{A_1}(a)$ are also calculated as Eqs. (9) and (10). Fig. 15 shows exceeding probabilities along the annual maximum PGA (A) and the PGA of one seismic event (A_1), and Fig. 16 shows the seismic hazard curve which represents the probability density function ($f_{A_1}(a)$) of the PGA (A_1) for each seismic event.

Combining seismic hazard $F_{A_1}(a)$, with the fragility curve $F_k(a)$, the seismic risk for the k^{th} damage state for one occurrence of earthquake (p_f^c), and for n -years ($p_f^{n\text{-yr}}$), can be evaluated using Eqs. (11) and (12).

Table 6 summarizes the results of seismic risks for one occurrence of earthquake, and several service years (in this study, 20, 50 and 100 years are considered) for the complete column collapse and superstructure damage cases. In the case of seismic damages on the column, only the complete damage is considered because this is the case of utmost concern. From the results, it can be concluded that the seismic risk can be reduced by introducing the seismic isolation devices about 10% of that of a typical bridge (i.e., from 2.7% to 0.3% for 20 years and from 6.6% to 0.6% for 50

Table 6 Seismic risk analysis results

Damage states		Service years				
		1 time	20 year	50 year	100 year	
Non-isolated bridges	Columns(collapse)	0.0005	0.0271	0.0664	0.1284	
	Behaviour of superstructure	0.0326	0.8261	0.9874	0.9998	
Seismically-isolated bridges	Columns(collapse)	0.0001	0.0030	0.0059	0.0118	
	Behaviour of superstructure	0.0439	0.9054	0.9972	1.0000	

years) while the seismic risk for a superstructure is a little bit increased from 80% to 90% for 20 years. Even though the excessive relative displacement of superstructure is a little bit increased, and the risk is almost 1.0 for 50 and 100 years, it can be considered as relatively small damages. The movement does not draw the catastrophic collapse of a bridge because the excessive displacement usually causes the damage for the supporting devices which can easily be replaced by new devices. Also, the unseating is not a problem since extradosed bridges are usually designed as a continuous girder system, and also the abutment size can be increased to prevent unseating. In this example bridge, the abutment is about 2 m and the gap between the abutment and bridge deck is about 0.4 m for preventing pounding. Therefore the relative displacement exceeding 1.6 m causes the unseating problem, and the 0.4-m relative displacement under a strong earthquake with 0.6 g of PGA can be ignored.

6. Conclusions

This paper presents a method for the probabilistic seismic risk assessment of a structure. First, the seismic vulnerability of a structure is evaluated in the form of seismic fragility curves using earthquake data set. Then, the seismic hazard of a given construction site is analyzed using available seismic hazard maps or others. Finally, the probabilistic seismic risk of the structure is assessed by combining the seismic vulnerability and seismic hazard.

This method is applied to evaluate the seismic risk for small and medium scaled earthquakes on an extradosed bridge with and without LRB seismic isolators. It is found that the seismic risk of an extradosed bridge can be reduced by adopting the LRB seismic isolators even though the bridge is relatively flexible and lightly damped. The following concluding remarks are drawn from the results of this study:

1. The exceeding damage probability for columns of an isolated bridge is much less than that of a typical bridge with the same service lives, and the seismic risk can be reduced to about 10% by introducing LRBs as supporting devices of a bridge.
2. The probability of seismic damage of superstructures is slightly increased by adopting the isolation devices up to a maximum of 30%. However, the excessive movement of a superstructure usually causes the damage for bearings which can easily be replaced by new ones after earthquakes.
3. The cables have not yielded under the earthquakes considered in this study, i.e. earthquakes with PGAs of under 0.6 g for an example bridge with and without seismic isolation devices. Therefore, the seismic fragility is not considered for the seismic cable damages. However, it is found that the axial force can be significantly reduced by installing LRBs.

4. Even though the LRBs have not been actively used as an effective tool to improve the seismic performance of flexible and lightly damped structures including extradosed bridges, it is verified that the LRBs can enhance the seismic performance and reduce the seismic risk of extradosed bridges by designing the LRBs carefully.

Acknowledgements

This work is a part of a research project supported by Korea Ministry of Construction & Transportation (MOCT) through Korea Bridge Design & Engineering Research Center at Seoul National University. The authors wish to express their gratitude for the financial support.

References

- AASHTO (1999), *Guide Specifications for Seismic Isolation Design*, 2nd Edition.
- Ali, H.M. and Abdel-Ghaffar, A.M. (1995), "Seismic passive control of cable-stayed bridges", *Shock Vib.*, **2**(4), 259-272.
- Ang, A.H.S. and Tang, W.H. (1975), *Probability Concepts in Engineering Planning and Design*, John Wiley & Sons.
- Computer and Structures, Inc. (2002), *SAP2000/Nonlinear Users Manual Version 8*, Berkeley, CA, USA.
- Chung, Y.S., Park, C.K. and Lee, D.H. (2006), "Seismic performance of RC bridge piers subjected to moderate earthquakes", *Struct. Eng. Mech.*, **24**(4), 429-446.
- Dutta, A. and Mander, J.B. (1998), "Seismic fragility analysis of highway bridges", in *Proc. of INCEDE-MCEER Center-to-Center Workshop on Earthquake Engineering Frontiers in Transportation Systems*, Tokyo, Japan, 311-25.
- Earthquake Engineering Society of Korea (1997), *Earthquake Resistant Design Standard Research (II)*, Ministry of Construction & Transportation.
- Elnashai, A.S. (2001), "Advanced inelastic static (pushover) analysis for earthquake applications", *Struct. Eng. Mech.*, **12**(1), 51-69.
- Farzad Naeim and James M. Kelly (1999), *Design of Seismic Isolated Structures from Theory to Practice*, John Wiley & Sons.
- Ghobarah, A. and Ali, N.M. (1988), "Seismic performance of highway bridges", *Eng. Struct.*, **10**, 157-166.
- Ghobarah, A., Aly, N.M. and El-Attar, M. (1997), "Performance level criteria and evaluation", *Proc. of the International Workshop on Seismic Design Methodologies for the next Generation of Codes*, Balkema, Rotterdam, 207-215.
- HAZUS (1997), "Earthquake loss estimation methodology", Technical Manual. *Prepared by National Institute of Building Science for Federal Emergency Management Agency*.
- Idriss, I.M. and Sun, J.I. (1992), *User's Manual for SHAKE91*, Center for Geotechnical Modeling, Department of civil and Environmental Engineering, University of California.
- Jacob, K.H. (1992), "Seismic hazards in the eastern U.S. and the impact on transportation lifelines", *Lifeline Earthquake Engineering in the Central and Eastern U.S.*, Monograph 5, ASCE, NY USA.
- Karim, Kazi, R. and Yamazaki, Fumio (2001), "Effect of earthquake ground motions on fragility curves of highway bridge piers based on numerical simulation", *Earthq. Eng. Struct. Dyn.*, **30**, 1839-1856.
- Kennedy, R.P. and Ravindra, M.K. (1984), "Seismic fragilities for nuclear power plant risk studies", *Nuclear Eng. D.*, **79**, 47-68.
- Kim, D.K. (2003), "Seismic isolated of structures", *Technical Articles at Korea Institute for Structural Maintenance Inspection*, **7**(4), 40-46.
- Kim, D.K., Seo, H.Y., Kim, S.H. and Yi, J.H. (2005), "Seismic fragility curves of extradosed bridges with lead rubber bearings", *Korean Soc. Civil Eng.*, **25**(2A), 429-435.

- Kim, S.H. and Shinozuka, M. (2004), "Development of fragility curves of bridges retrofitted by column jacketing", *Probabilistic Eng. Mech.*, **19**(1/2), 105-112.
- Korean Society of Civil Engineers (2005), *Korea Bridges Design Code*, Ministry of Construction & Transportation.
- Priestley, M.J.N., Seible, F. and Calvi, G.M. (1996), *Seismic Design and Retrofit of Bridges*, John Wiley & Sons, Inc, 270-273.
- Rechart, F.E., Woods, R.D. and Hall, J.R. (1970), *Vibrations of Soils and Foundations*, Prentice-Hall.
- Shinozuka, M., Feng, M.Q., Kim, H.K. and Ueda, T. (2002), "Statistical analysis of fragility curves", *Technical Report at Multidisciplinary Center for Earthquake Engineering Research*, NY, USA.
- Shinozuka, M., Feng, M.Q., Lee, J. and Naganuma, T. (2000), "Statistical analysis of fragility curves", *J. Eng. Mech.*, ASCE, **126**(12), 1224-1231.
- Shinozuka, M., Hwang, H. and Reich, M. (1984), "Reliability assessment of reinforced concrete containment structures", *J. Eng. D.*, **80**, 247-267.
- Su, R.K.L., Chandler, A.M., Li, J.H. and Lam, N.T.K. (2002), "Seismic assessment of transfer plate high rise buildings", *Struct. Eng. Mech.*, **14**(3), 287-306.
- UCFyber Users Manual (2001), Imbsen & Associates, Inc., Berkeley, CA, USA.
- Vanmarcke, E.H. and Gasparini, D.A. (1976), "A program for artificial motion generation, user's manual and documentation", Department of Civil Engineering, MIT.
- Yun, C.B., Choi, J.S. and Kim, J.M. (1999), "Identification of the Hualien soil-structure interaction system", *Soil Dyn. Earthq. Eng.*, **18**, 395-408.